2023 IMEKO TC-4 International Conference on
Metrology for Archaeology and Cultural Heritage
Rome, Italy, October 19-21, 2023

# Wireless Sensing of Permittivity for Cultural Heritage Monitoring Using a Passive SRR

Erika Pittella[1], Andrea Cataldo[2], Marta Cavagnaro[1], Livio D'Alvia[3], Francesco Fabbrocino[4], Emanuele Piuzzi[1]

*[1] Department of Information Engineering, Electronics and Telecommunications, Sapienza University of Rome, Rome, Italy, {erika.pittella, marta.cavagnaro, emanuele.piuzzi}@uniroma1.it*
*[2] Department of Engineering for Innovation, Complesso Ecotekne-Corpo O, University of Salento, Lecce, Italy; andrea.cataldo@unisalento.it*
*[3] Department of Mechanical and Aerospace Engineering, Sapienza University of Rome, Rome, Italy, livio.dalvia@uniroma1.it*
*[4] Pegaso University, Naples, Italy; francesco.fabbrocino@unipegaso.it*

***Abstract* – Monitoring water content in cultural heritage materials through non-invasive and easy-to-use measurement systems allows the enhancement of artistic patrimony conservation activities. In this study, the response of a passive split ring resonator (SRR) used to monitor the dielectric characteristic of a material under test, when excited through an antipodal Vivaldi antenna operating close to the resonator, is analyzed through numerical simulations and then assessed by measurements. Our results reveal the possibility of monitoring the moisture content in materials largely used in artistic artifacts, such as wood and stone, through measurements of the SRR resonance frequency, which is directly related to material dielectric characteristics.**

## I. INTRODUCTION

The conservation of cultural heritage comprises the actions taken to extend the life of artistic patrimony. In the domain of cultural property, conservation aims to maintain the physical and cultural characteristics of the object, in order to ensure that its value is not diminished [1]. One of the objectives that arises in the topic of cultural heritage monitoring (such as paintings, and wooden and stone structures) is the possibility of implementing and using low-cost wireless systems for remote sensing [2]. Among different devices, planar microwave sensors based on resonators resulted in a promising approach, that offers compactness, accurate sensing, and durability, to reveal small material changes through the shift in the resonance frequency when the resonator is placed near a material under test (MUT) [3, 4]. In particular, split ring resonators (SRRs) have been largely utilized in the field of sensing, thanks to their simple and compact design and ease of manufacture [5-6].

In this context, it would be interesting to investigate wireless and contactless sensing using a portable and light antenna coupled to the SRR, studying the variation of the $S_{11}$ response of the antenna, due to the SRR resonance shift, for a material under test with varying permittivity and loss tangent. This idea has been previously investigated in [7] and [8] for remote liquid sample interrogations.

In this paper, a simple groundless SRR tag is studied and designed to interact with a compact antenna reader. The proposed design of the SRR was based on previous works using low-cost substrates and effective ring geometry [9, 10]. The chosen sensing antenna is an antipodal Vivaldi antenna designed to be compact and lightweight [11].

## II. MATERIAL AND METHODS

### *A. Planar Resonator Design*

The design of the resonator was performed using CST Studio Suite by Simulia [12]. In particular, a circular groundless planar SRR was chosen to be used in contact with the material, starting from the SRR geometry proposed in [4] and studying the antenna response behavior in terms of resonance frequency without the SRR ground (Fig. 1a). The ground was removed to allow interrogation of the tag from behind, once the SRR is placed with its upper face in contact with the artistic artifact to be monitored. To find the SRR resonance frequencies, the Eigen Mode Solver was used. It calculates the frequencies and the corresponding electromagnetic field patterns (eigenmodes) when no excitation is applied.

The final idea is to use the system with a portable and low-cost VNA [13, 14]. This kind of device has a typical band not exceeding 3 GHz, therefore we concentrated the study of the modes below this frequency. We found two principle modes around 0.9 GHz ($Q_{TOT}$ = 102) and 1.7 GHz ($Q_{TOT}$ = 165), as shown in Fig. 2.

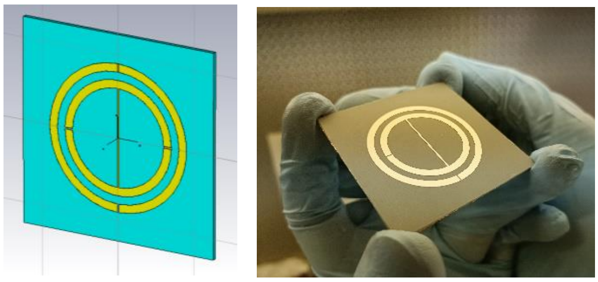

(a) (b)

*Fig. 1. SRR geometry (a) and a picture of the fabricated SRR prototype (b).*

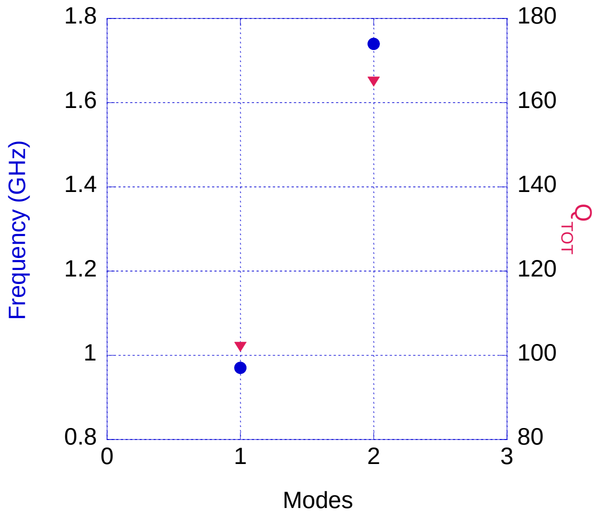


*Fig. 2. Resonance frequencies (circles) and $Q_{TOT}$ (triangles) of the two principal modes.*

### *B. Principle of Operation*

The system schematic implemented with CST is shown in Fig. 3 and it comprises a circular groundless SRR, an antipodal Vivaldi transceiver antenna, and a MUT placed near the gap of the resonator, which is the most sensitive region. The antenna was positioned close to the SRR to guarantee the operation of the sensor in the antenna reactive near field. In this region, the antenna field is sensitive to the EM absorption and this affects its reflection coefficient and input impedance [8].

### *C. Sample types*

The measurements were conducted on four different wood species: (i) fir, (ii) poplar, (iii) beech, and (iv) oak. All samples have the following transversal dimensions: 22.86 mm × 10.16 mm.

First, the dried sample was measured through a 10-mg resolution electronic balance, and the response of the antenna in the presence of the sample was acquired with a VNA. Then, the sample was bathed in deionized water for some minutes and then measured at two different humidity levels. The gravimetric water content (θ%) was calculated according to (1):

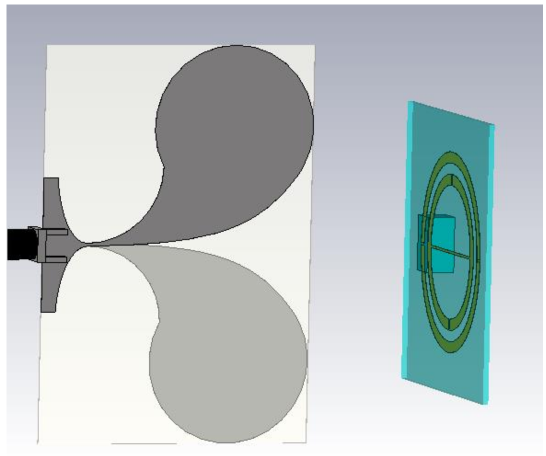

*Fig. 3. Scheme of the antenna interrogating the SRR tag.*

$$\theta(\%) = \frac{Wi - Wdry}{Wi} \times 100; \qquad (1)$$

where $W_i$ is the mass of the moist specimen and $W_{dry}$ is the mass of the dried sample. The steps of the measurement procedure are similar to those detailed in [13-16].

To test the proper functioning of the system on materials other than wood, similar measurements were also carried out on a sample of Gentile stone (with the same transversal dimensions of the wooden samples), typically found in Cultural Heritage structures in Southern Italy and particularly affected by deterioration and decay phenomena.

## III. NUMERICAL RESULTS

EM simulations were conducted with the transceiver antenna and the passive groundless SRR electromagnetically coupled, while a MUT was placed near the gap region. In particular, dielectric properties variation near the resonator gap changes the SRR resonance frequency and, due to the EM coupling, the antenna input impedance and therefore its $S_{11}$. Fig. 4 shows the simulated reflection coefficient of the antenna. To enhance the effect of the SRR the antenna orientation was chosen so as to create an electric field parallel to the SRR gap (see Fig. 3). In these first simulations, the permittivity of the MUT was varied from 1 to 9 in steps of 2.

As we expected, the first two resonances (when $\varepsilon_{MUT}$ = 1) are present around 0.88 GHz and 1.72 GHz, in accordance with the Eigen Mode simulation results. In particular, as expected, if the permittivity of the MUT increases the resonance frequency decreases. If the copper part of the passive SRR is not present in the simulation, the $S_{11}$ presents a wideband behavior similar to the return loss of the antenna in air with no substantial changes when the permittivity of the MUT varies (Fig. 5). This proves that the observed resonances in the $S_{11}$ are those of the SRR.

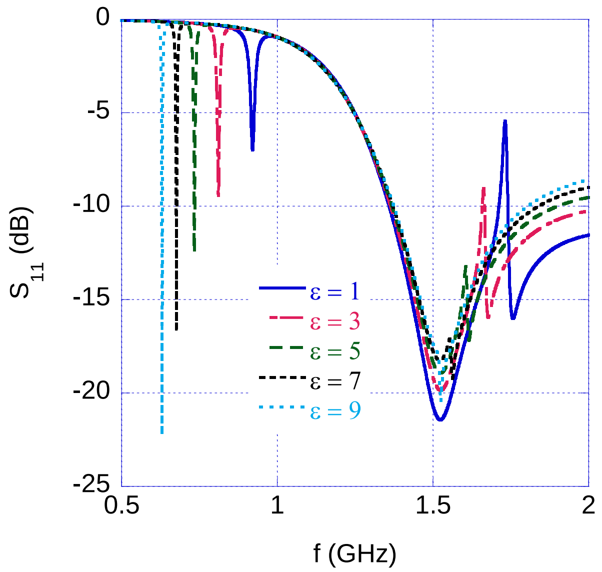


*Fig. 4. $S_{11}$ of the antenna in front of the SRR placed on a MUT with varying permittivity.*

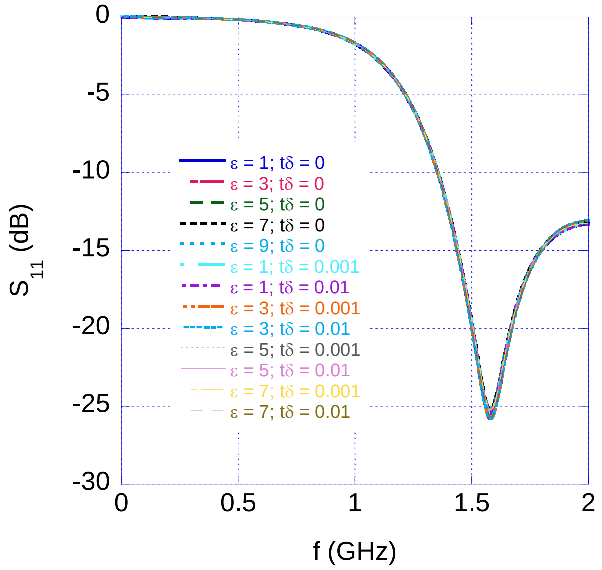


*Fig. 5. $S_{11}$ of the antenna in front of the MUT with no SRR.*

Based on the numerical results, considering the first resonance of the SRR, the calibration curve $f_r \rightarrow \varepsilon_r$ was extrapolated (see Fig. 6).

Therefore, to compute the dielectric constant, starting from the measured resonance frequency $f_r$, the following relation can be applied:

$$\varepsilon = 58.366 - 113.36 \cdot f_r + 55.486 \cdot f_r^2 \tag{2}$$

## IV. MEASUREMENTS

Measurements are performed using the Agilent E8363C VNA.

### A. Measurements on known samples

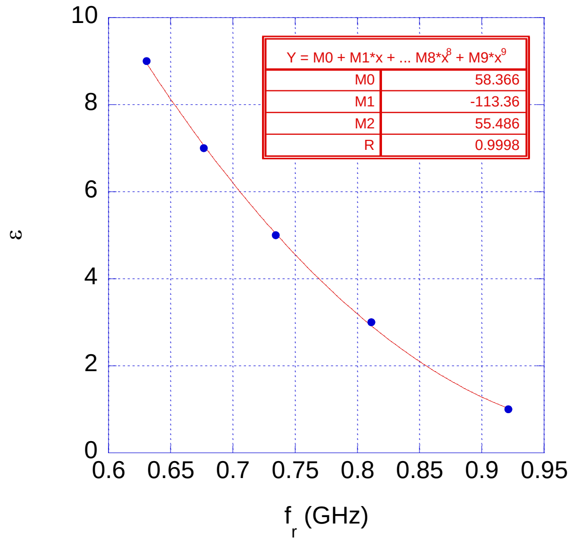


*Fig. 6. $f_r \rightarrow \varepsilon_r$ relationship.*

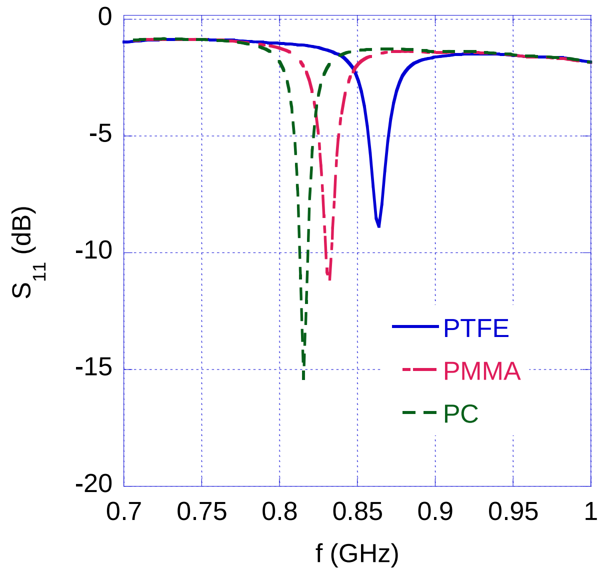


*Fig. 7. Measured $S_{11}$ of the antenna in front of the SRR placed in contact with the known samples.*

The calibration curve obtained through the EM simulations is first experimentally verified by testing the system on well-known materials, previously characterized in [5]: PTFE, PMMA, and PC. The antenna response in the presence of these materials is shown in Fig. 7.

Table I displays the measured resonance frequency, the permittivity computed using (2), and the permittivity of the same sample characterized with the WR90 in [5]. The maximum relative error is below 10%. It must also be evidenced that the calibration curve is sensitive to the dimensions of the sample and part of the observed error can be attributed to the fact that the experimental sample dimensions were not perfectly coincident with those of the simulated sample.

Table I. Permittivity of test materials computed with the proposed system and comparison with reference data.

| Material | $f_r$ (GHz) | $\varepsilon_r(f_r)$ | $\varepsilon_r$ [5] |
|---|---|---|---|
| PC | 0.81543 | 2.82 | 2.82 |
| PMMA | 0.83225 | 2.46 | 2.59 |
| PTFE | 0.86402 | 1.84 | 2.06 |

*B. Measurements on typical cultural heritage materials.*

Experiments were performed on the wood samples described in Section II.C.

Fig. 8. shows the antenna response on one of the wood samples, i.e. beech. For the other samples, a similar behavior of the $S_{11}$ was obtained.

Table II summarizes the moisture content for the four kinds of wood analyzed in the measurements.

Fig. 9 shows the resulting calibration curve. For subsequent moisture content measurements, it suffices to evaluate the $f_r$ value and to infer the corresponding value of θ through the calibration curve.

Similar calibration curves are obtained for the other wood samples and are shown below:

| | | |
|---|---|---|
| $\theta = 118 - 1.4592e\text{-}7\ f_r$ | R= 0.99885 | beech |
| $\theta = 319.05 - 3.7006e\text{-}7\ fr$ | R= 0.96621 | fir |
| $\theta = 155.35 - 1.8663e\text{-}7\ fr$ | R= 0.99996 | poplar |
| $\theta = 145.61 - 1.7937e\text{-}7\ fr$ | R= 0.99994 | oak |

It is worth noting that the linear fit shows a lower correlation coefficient for fir samples. This is due to the high water contents reached with this sample, which are probably outside of the linear range. On the other hand, realistic water contents expected in a cultural heritage scenario are much lower.

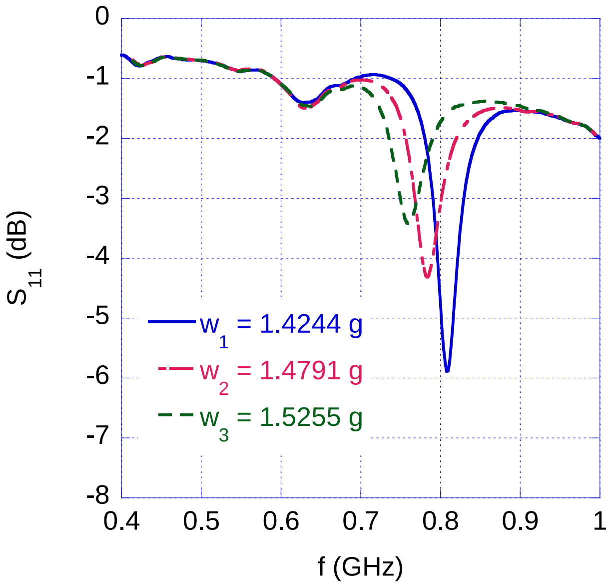


*Fig. 8. $S_{11}$ behavior for the beech sample at different moisture content: $w_1$ is the weight of the dry wood while $w_2$ and $w_3$ are weights of the moistened sample.*

Table II. Gravimetric water content of the tested samples.

| Material | $\boldsymbol{\theta_2}$(%) | $\boldsymbol{\theta_3}$ (%) |
|---|---|---|
| beech | 3.840 | 7.09 |
| fir | 22.72 | 25.00 |
| oak | 4.09 | 7.37 |
| poplar | 8.13 | 14.29 |

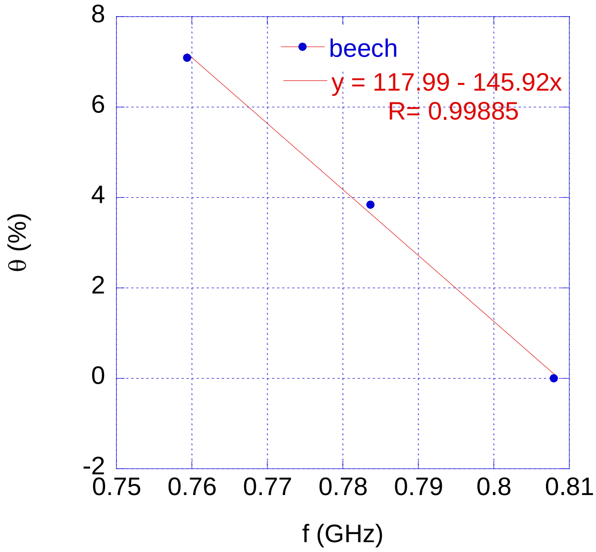


*Fig. 9. Calibration curve for θ measurements on beech samples.*

All calibration curves will be improved in the future considering a larger set of gravimetric water contents.

Finally, the system was successfully tested in the presence of a Gentile stone sample. The results of the antenna response are shown in Fig. 10 and the corresponding calibration curve is $\theta = 18.023 - 2.5603e\text{-}8\ f_r$ R= 0.97601.

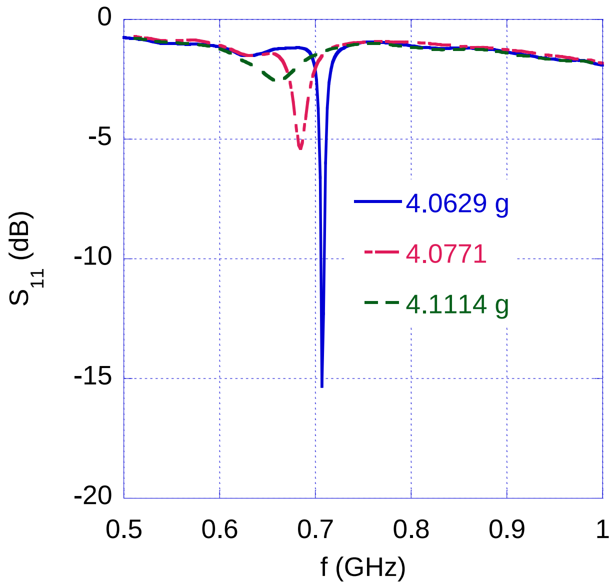


*Fig. 10. $S_{11}$ behavior for the Gentile stone at different moisture content.*

## V. CONCLUSIONS

In this work, a system for monitoring moisture content in cultural heritage materials was presented. The proposed system resorts to the evaluation of the moisture content from measurements of an antenna return loss placed near a passive split ring resonator in contact with the material under test. Measurements were carried out on four types of wood, and a stone sample. Corresponding calibration curves were derived. In practical applications, these calibration curves can be used to automatically retrieve the value of moisture content from resonance frequency measurements. The advantage of the proposed system is that it allows monitoring of the water content of materials directly on-site by measuring the response of the antenna with a portable and low-cost VNA.

Future developments will include expanding the set of tested materials, improving the calibration curves, and possibly including also the effect of sample size.

Moreover, experimental results evidence that as the water content increases the resonance frequency decreases and, at the same time, the Q decreases as well. It would be interesting to assess whether using both the resonance frequency and the Q value as input data the accuracy of water content evaluation can be improved.

## VI. ACKNOWLEDGMENTS

The authors wish to thank Dr. Alessio Buzzin for his support in SRR manufacturing.

## REFERENCES

[1] UNESCO Institute for Statistics, 2009 UNESCO Framework for Cultural Statistics and International Centre for the Study of the Preservation and Restoration of Cultural Property (ICCROM), Risk Preparedness: A Management Manual for World Cultural Heritage, 1998 and; UNESCO, Traditional Restoration Techniques: A RAMP Study, 1988.

[2] M.C. Rodriguez-Sanchez, S. Borromeo and J.A. Hernández-Tamames, "Wireless Sensor Networks for Conservation and Monitoring Cultural Assets," in IEEE Sensors Journal, vol. 11, no. 6, pp. 1382-1389, June 2011.

[3] E. Pittella, L. Angrisani, A. Cataldo, E. Piuzzi and F. Fabbrocino, "Embedded Split Ring Resonator Network for Health Monitoring in Concrete Structures," in *IEEE Instrumentation & Measurement Magazine*, vol. 23, no. 9, pp. 14-20, December 2020.

[4] E. Pittella, R. Schiavoni, G. Monti, A. Masciullo, M. Scarpetta, A. Cataldo, E. Piuzzi, "Split Ring Resonator Network and Diffused Sensing Element Embedded in a Concrete Beam for Structural Health Monitoring", *Sensors* 2022, *22*, 6398.

[5] A. Alimenti, E. Pittella, K. Torokhtii, N. Pompeo, E. Piuzzi and E. Silva, "A Dielectric Loaded Resonator for the Measurement of the Complex Permittivity of Dielectric Substrates," in *IEEE Trans. Instr. Meas.*, vol. 72, pp. 1-9, 2023, Art no. 6001009.

[6] Y. Xie, X. Yang, H. Xiao, Y. Wang, "A split-ring resonator probe for assessing subsurface wood defects". The Review of scientific instruments, 90(12), 125004, 2019.

[7] S. Karuppuswami, A. Kaur, M.I.M. Ghazali, and P. Chahal, "RFID compatible sensor tags for remote liquid sample interrogation," in Proc. IEEE 66th Electron. Compon. Technol. Conf. (ECTC), May/Jun. 2016, pp. 2401–2407.

[8] B.D. Wiltshire, T. Zarifi and M.H. Zarifi, "Passive Split Ring Resonator Tag Configuration for RFID-Based Wireless Permittivity Sensing," in IEEE Sensors Journal, vol. 20, no. 4, pp. 1904-1911, 15 Feb.15, 2020.

[9] R.A. Alahnomi, Z. Zakaria, E. Ruslan, S.R. Ab Rashid, and A.A. Mohd Bahar, "High-Q Sensor Based on Symmetrical Split Ring Resonator with Spurlines for Solids Material Detection," in IEEE Sensors Journal, vol. 17, no. 9, pp. 2766-2775, 1 May 1, 2017.

[10] E. Pittella, E. Piuzzi, "Split ring resonator for complex permittivity measurement", 24th IMEKO TC4 International Symposium and 22nd International Workshop on ADC and DAC Modelling and Testing Pages 85 - 892020, IWADC 2020, Palermo, 14 - 16 September 2020.

[11] N. Zeni, G. Bellizzi, L. Crocco and M. Cavagnaro, "A Compact Antipodal Vivaldi Antenna for Food Investigation," 2023 17th European Conference on Antennas and Propagation (EuCAP), Florence, Italy, 2023, pp. 1-4.

[12] https://www.3ds.com/products-services/simulia/products/cst-studio-suite/

[13] A. Cataldo, E. De Benedetto, G. Cannazza, E. Piuzzi, and E. Pittella, "TDR-Based Measurements of Water Content in Construction Materials for In-the-Field Use and Calibration," in IEEE Transactions on Instrumentation and Measurement, vol. 67, no. 5, pp. 1230-1237, May 2018.

[14] L. D'Alvia, E. Pittella, E. Rizzuto, E. Piuzzi, Z. Del Prete, "A portable low-cost reflectometric setup for moisture measurement in cultural heritage masonry unit,", Measurement, vol. 189, 2022.

[15] L. D'Alvia, E. Piuzzi, A. Cataldo, and Z. Del Prete, "Permittivity-Based Water Content Calibration Measurement in Wood-Based Cultural Heritage: A Preliminary Study," Sensors, vol. 22, no. 6, p. 2148, Mar. 2022.

[16] L. D'Alvia, E. Piuzzi, A. Cataldo, and Z. Del Prete, "Permittivity of wood as a function of moisture for cultural heritage applications: a preliminary study", Journal of Physics: Conference Series, Volume 2204, 2021.